Supporting Information. Amandine Gamble, Romain Garnier, Thierry Chambert, Olivier Gimenez and Thierry Boulinier. 2019. Next-generation serology: integrating cross-sectional and capture-recapture approaches to infer disease dynamics. *Ecology*.

Appendices S1. Supplementary text and figures

Section S1. Additional details on the methods

Eco-epidemiological model and parameterization

Individual data resulting from an eco-epidemiological inter-annual process were simulated with a set of parameters being fixed to different values depending on various scenarios. Those parameters were the annual survival (ϕ), seroconversion (λ) and seroreversion (ω) probabilities. Among vertebrates, an annual survival probability around 0.5 or less corresponds to short-lived species like passerine birds (Grosbois et al. 2006) while an annual survival probability around 0.8 or more corresponds to long-lived species like seabirds or bats (e.g., Chambert et al. 2012, Robardet et al. 2017, Gamble et al. 2019a). In the simulations, we explored values between 0 and 1. An annual seroreversion probability close to zero corresponds to a long-lived immunity (e.g., immunity against the Newcastle disease virus vaccine in Ramos et al. 2014) while an annual seroreversion probability close to one corresponds to a short-lived immunity (e.g., immunity against the avian cholera agent in Samuel et al. 2003). Intermediate values of the annual seroreversion probability are also observed in natural systems (e.g., immunity against

the parasite *Toxoplasma gondii* in waterfowl in Sandström et al. 2013). In the simulation, we explored a range of values between 0 and 1 (see details on the figures).

Regarding the exposure of individuals to the infectious agent, in the simulations, exposure was set to occur during a short time period, which can for example correspond to the breeding season for colonial species, when individuals are gathered on the breeding ground where the infectious pressure can be higher than on the wintering sites (e.g., in the case of a tick-born infectious agent transmitted to seabirds on the breeding ground but not on the wintering area). Within a time step, samples were set to be collected after exposure but before waning of the produced antibodies; this assumption should be met when individuals are sampled late in the breeding season, for example during the offspring rearing period, which is generally the case for colonial breeders as adults are easier to capture during this period. Individuals were set to recruit in the population as seronegative, which can be expected for a wide range of infectious agents considering the contrasted life styles of juveniles and adults of various species. An extreme example is seabirds and pinnipeds, which spend most of their early life at sea and return on land (where they can be exposed to various infectious agents) to breed only several years after their emancipation.

To illustrate how eco-epidemiological parameters could be quantified from serological data, we have chosen the simple situation of populations at the demographic and endemic equilibrium (*i.e.*, recruitment compensates mortality and the seroprevalence is stable over time; Hens et al. 2012) with exposure having no impact on survival or detectability. The population size was fixed at 600 individuals, which can for instance represent a population of birds nesting in a cliff or bats in roosts (e.g., Ponchon et al. 2014). Sampling was conducted after the endemic equilibrium was reached (Fig. S1). Resighting and recapture probabilities can vary depending on many factors, but for site faithful species like seabirds and bats, high resighting or recapture probabilities (around 0.8) can commonly be reached (e.g., Chambert et al. 2012). For the simulations, unless otherwise stated, those parameters were thus set to 0.80.

Simulation outputs

An example of the outputs of the eco-epidemiological simulations is provided in Fig. S1 and an extract of the simulated data obtained for marked individuals is presented in Table S1.

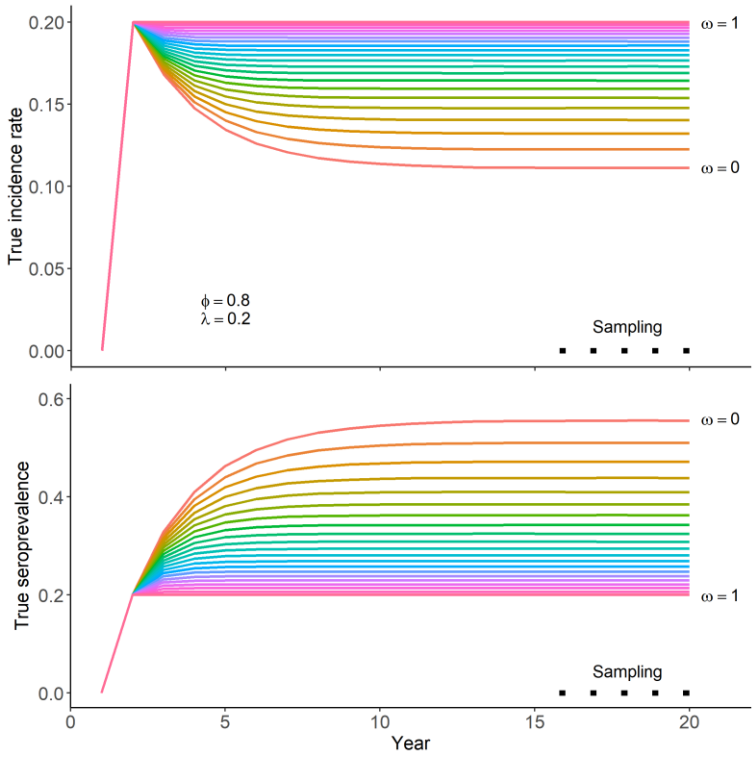

FIGURE S1. Example of the outputs of the eco-epidemiological simulations: temporal change of the incidence rate and of the seroprevalence in simulated populations for different values of the seroconversion probability (ω). Note that the incidence rate (proportion of newly infected individuals in the whole population) is not to be confused with the force of infection (rate at which susceptible individuals become infected). The force of infection can often be approximated by the seroconversion rate (rate at which seronegative individuals become seropositive). For a fixed force of infection (or seroconversion rate), the incidence will vary depending on the proportion of susceptible (or seronegative) individuals in the population.

TABLE S1. Extract of the simulated data obtained for marked individuals. ind = individuals identity; year = year since the beginning of the simulation; exposed = indicates if the individual seroconverted a given year; seropositive = individual serological status; marked = indicates if the individual has been marked before; resighted = indicates if the individual has been resighted a given year; sampled = indicated if the individual has been captured (*i.e.*, individual serological status has been ascertained) a given year; event = individual observation state in the capture-mark-recapture history matrix. Individuals that do not seroconvert a given year but are seropositive (e.g., ind 813) correspond to individuals that seroconverted previously and maintained detectable antibody levels over the years. Individual recorded as not resighted but sampled a given year (e.g., ind 813) correspond to newly marked individual this year. An observation event was then attributed each year to each marked individual of the study and recorded in the matrix *m*: 0 if not seen, 1 if ascertained as seronegative, 2 if ascertained as seropositive or 3 if seen but not captured (serological state uncertain).

ind	year	exposed	seropositive	resighted	marked	sampled	event
443	17	0	0	0	1	0	0
470	17	0	0	1	1	0	3
696	17	0	0	1	1	1	1
769	17	0	0	1	1	1	1
813	17	0	1	0	1	1	2
851	17	1	1	0	1	1	2
871	17	0	1	1	1	1	2
873	17	0	0	1	1	1	1
900	17	0	1	0	1	1	2
906	17	0	1	1	1	1	2
918	17	0	0	0	1	0	0
937	17	0	0	1	1	1	1
955	17	0	0	0	1	1	1
1053	17	0	0	1	1	1	1
1070	17	0	1	1	1	1	2
1072	17	1	1	1	1	1	2
1093	17	0	0	1	1	0	3
1118	17	1	1	0	1	1	2
1142	17	0	1	1	1	0	3

Cross-sectional sampling and binomial model

Each year, n_{CS} individuals are randomly captured and sampled for serological analyses.

Following equation 1 and at the demographic equilibrium, recruitment compensates for mortality and r can be written as $(1 - \phi)$:

$$\pi_{t+1} = \pi_t \phi (1 - \omega) + \pi_t \phi \omega \lambda + (1 - \pi_t) \phi \lambda + (1 - \phi) \lambda \quad \text{(S1)}$$

Following equation S1 and at the endemic equilibrium, the seroprevalence is constant ($\pi_{t+1} = \pi_t$) and its value (π^*) is thus given by:

$$\pi^* = \pi^* \phi (1 - \omega) + \pi^* \phi \omega \lambda + (1 - \pi^*) \phi \lambda + (1 - \phi) \lambda \quad \text{(S2)}$$

$$\pi^* = -\frac{\lambda}{\phi (1-\omega + \omega \lambda-\lambda)-1} \quad \text{(S3)}$$

The observed sample states (seronegative or seropositive; regrouped in the vector y) thus follow a hypergeometric distribution approximated by a binomial distribution (B) with the probability for a sample to be seropositive corresponding to the seroprevalence π^* (equation S4).

$$y \sim B\left(n_{CS}, -\frac{\lambda}{\phi (1-\omega + \omega \lambda-\lambda)-1}\right) \quad \text{(S4)}$$

As the seroprevalence (π^*) can be expressed as a function of the seroconversion, the survival and the seroreversion probabilities, these parameters can be estimated by maximizing the likelihood and estimations of unknown parameters will be facilitated if one or two of the other parameters is known *a priori* (notably because several combinations of the three parameters can lead to the same seroprevalence at the equilibria; Fig. S2). In this study, we thus considered the case when the model was informed with some values for the survival and the seroreversion probabilities (true or erroneous). Annual survival probabilities are for instance available in the literature for an increasing number of study systems. Persistence of antibody levels in wild host species is generally inferred from what is known in domestic animals or from experimental settings (Hénaux et al. 2010, Pepin et al. 2017), which can lead to consider a fast waning of antibody level (e.g., Samuel et al. 2005) or lifelong persistence (e.g., Garnier et al. 2014).

The benefit of the approximation by a binomial distribution rather than using a hyper-geometric distribution is that the statistical population size (N) does not need to be known or estimated; this approximation can reasonably be made when $n_{CS}/N < 0.10$.

Longitudinal sampling and multievent capture-recapture model

The observation process is illustrated in Fig. S2. The "uncertain" state corresponds to individuals that were seen but not captured nor sampled; the "Sero.−" and "Sero.+" states correspond to individuals that were seen, sampled and determined as seronegative and seropositive respectively based on the serological analyses run on its sample. Examples of individual histories are given in Table S1.2. Note that the number of resighting and recapture events for each individual is not fixed but will depend on the survival, resighting and recapture probabilities. For instance, within a five-year study with an annual sample size maintained at 50 individuals, for $\phi = 0.8$, $p = 0.8$ and $\delta = 0.8$ (cliff-nesting seabird type), 115 individuals were marked and each individual was seen on average (± standard deviation) 2.5 ± 1.3 times and captured 2.2 ± 1.1 times; for $\phi = 0.5$, $p = 0.8$ and $\delta = 1.0$ (cavity-nesting passerine type), 158 individuals were marked and each individual was seen and captured 1.6 ± 0.9 times.

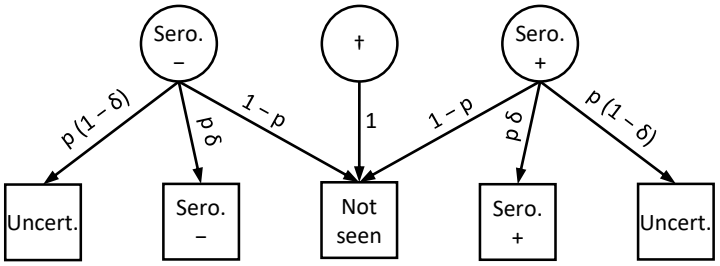

Individual states
Sero.− = seronegative
Sero. + = seropositive
† = dead
Observation parameters
p = resighting probability
δ = recapture probability

Individual events
Not seen = not seen
Sero.− = seen, captured and ascertained as seronegative
Sero. + = seen, captured and ascertained as seropositive
Uncert = uncertain (*i.e.*, seen but not captured and not tested)

FIGURE S2. Observation process for the multievent capture-recapture model. Circles denote individual states; squares denote individual observation events.

Table S2. Example of capture-recapture individual histories. ind = individuals identity; occasions 1 to 5 = observation events recorded during five observation occasions. Observation events are recorded as 0 if not seen (because it is dead or alive but not present or not present but not detected in the study site), 1 if ascertained as seronegative, 2 if ascertained as seropositive or 3 if seen but not captured (uncertain serological state). Parameters were set at: $\phi = 0.8$; $\lambda = 0.3$; $\omega = 0.4$; $p = 0.8$; $\delta = 0.8$. For instance, individual 1068 was marked during the first occasion (and ascertained as seropositive) but not resighted during the third occasion although it was still alive as it was resighted during the following occasion (and ascertained as seronegative). Individual 1047 was marked during the third occasion (and ascertained as seropositive) and resighted but not recapture during the following occasion.

ind	occasion 1	occasion 2	occasion 3	occasion 4	occasion 5
24	2	2	2	2	0
479	2	3	2	0	0
734	0	0	0	0	2
843	0	2	2	2	2
863	1	0	1	2	3
1021	1	3	1	3	0
1040	0	1	1	2	2
1047	0	0	2	3	0
1056	2	2	0	2	1
1069	2	2	0	1	3
1093	1	1	3	0	0
1104	0	1	1	0	0
1126	0	2	0	0	2
1140	0	1	0	0	0
1147	0	2	2	0	0
1151	1	0	0	0	0
1180	1	1	0	0	0
1238	0	0	0	2	2
1270	0	0	0	0	1
1379	0	0	0	1	1

The following matrices are used to model the capture-recapture initial state and state and event processes in a multievent framework:

Initial state

$$[1-\pi \quad \pi \quad 0]$$

State process

1. Survival matrix

$$\begin{bmatrix} \phi & 0 & 1-\phi \\ 0 & \phi & 1-\phi \\ 0 & 0 & 1 \end{bmatrix}$$

2. Transition matrix

$$\begin{bmatrix} 1-\lambda & \lambda & 0 \\ \omega-\omega\lambda & 1-\omega+\omega\lambda & 0 \\ 0 & 0 & 1 \end{bmatrix}$$

Event process

1. Observation matrix

$$\begin{bmatrix} 1-p & p & 0 \\ 1-p & 0 & p \\ 1 & 0 & 0 \end{bmatrix}$$

2. Capture matrix

$$\begin{bmatrix} 1 & 0 & 0 & 0 \\ 0 & \delta & 0 & 1-\delta \\ 0 & 0 & \delta & 1-\delta \end{bmatrix}$$

Assumptions

In the present study, a binomial model was fitted to the seroprevalence data and a multievent model to the individual histories. Classical assumptions corresponding to these models had to be made. Here, we present some of the main assumptions made by the presented integrated model and how to relieve them.

(1) Dispersal is negligible in the considered compartment of the population (e.g., breeders). This assumption is often made in capture-recapture studies focusing on a unique site. Ideal setups should consider several sites and buffer zones to account for dispersal (Ponchon et al. 2018). The integrated approach could in theory be adapted to multisite setups on the condition that enough data are available to fit a multievent model including as many states as necessary to account for the two serological states and the multiple sites.

(2) The positivity threshold of the serological test is known. Determination of the positivity threshold for immunoassays in wild species has long been considered as a challenge, notably because of the lack of individuals of known status (no negative and/or positive controls; Gilbert et al. 2013). Recent advances have however made available statistical methods for the estimation of positivity thresholds based on the data distribution prior to the model fitting (e.g., Garnier et al. 2017) or within the modelling framework (e.g., Choquet et al. 2013a). These methods are however not perfect and may lead to state misclassification (see below).

(3) There is no state misclassification (test sensitivity and specificity equal to one). Different approaches can be used to account for potential misclassification. Their implementation required adapted sampling designs such as repeated sampling (Lahoz-Monfort et al. 2016) or combined tests (Buzdugan et al. 2017).

(4) The population is at the demographic equilibrium, hence recruitment compensates mortality. As for most statistical models, an assumption has to be made on recruitment but different assumptions can explored by modifying the relation linking the seroprevalence at times t (π_t) and t+1 (π_{t+1}; equation 1) accordingly.

(5) The population is at the endemic equilibrium, hence the seroprevalence is constant over time. To account for variations of seroprevalences, the relation linking the seroprevalence at times t (π_t) and t+1 (π_{t+1}; equation 1) can be conserved and treated as

a linear function (instead of considering that π^* is constant across sampling occasions and that it follows a binomial or a hypergeometric distribution). The intercept and slope of this function (which are themselves functions of λ, ω and ϕ; see equation 1) can then be estimated by maximization of the likelihood or by Bayesian inference (e.g., Samuel et al. 2015).

(6) The estimated parameters are homogeneous among the study population (survival, seroconversion, seroreversion, resighting and capture probabilities). The presented models could be modified to account for individual variables (e.g., differences in seroconcervation probabilities linked to sex or age class; e.g., Robardet et al. 2017), state dependent parameters (e.g., differences in survival probabilities as a consequence of disease-induced mortality; e.g., Chambert et al. 2012), time dependent parameters (e.g., variations in the seroconversion rate as a consequence of fluctuations of the size of a vector population; Chambert et al. 2012) or impacts of random effects on the transition probabilities (e.g., family effect; Choquet et al. 2013b). In these cases, the matrices of the capture-recapture model and the equation describing the temporal variations of seropravalence should be written as dependent on the considered factor(s) (individual variables, state, time or random effect). For instance, in the presented model, the state transition probability is state dependent ($\lambda \neq \omega$).

(7) Seroprevalence follow a binomial distribution. As mentioned above, The benefit of the approximation by a binomial distribution rather than using a hyper-geometric distribution is that the statistical population size (N) does not need to be known or estimated; this approximation can reasonably be made when $n_{CS}/N < 0.10$. Note that population size could potentially be estimated using capture-recapture data (Williams et al. 2002 for a review), and by extension, the presented integrated framework.

(8) The cross-sectional and longitudinal datasets are independent. As this assumption is typical from integrated models, it is discussed in detail below.

Note however that choosing different models (among the available capture-recapture models or by formalizing differently the variations of seroprevalences) would lead to different assumptions as mentioned above and in the discussion in the main text.

Integrated model and the assumption of independence of the datasets

Typically, integrated models rely on the assumption that the datasets are independent (Besbeas et al. 2002) and a higher accuracy of the estimators is expected for two fully independent datasets. Violation of this independence assumption has nevertheless been shown to have a very limited impact on estimator bias and precision in a demographic context (Abadi et al., 2010), but this is something to keep in mind. If data from only unmarked individuals are included in the cross-sectional dataset, which can easily be the case when samples are collected from captured individuals, both data sets should be completely independent. Conversely, it can sometime be difficult to observe the mother of a given offspring at the time of sampling (for instance when eggs are left alone in their nest, or nestlings in crèches, in the case of birds, or pups onshore in the case of pinnipeds). Thus, when offspring are sampled to get information on their mothers' serological state, it then could lead to some sampled individuals being represented in both datasets (the offspring as part of the cross-sectional sampling, and its mother as part of the longitudinal sampling, both samples containing information on the serological status of the mother). It may nevertheless concern only a minor part of the samples as for instance in site faithful species breeding sites locations can be marked and thus offspring of marked individuals excluded from the cross sectional sampling. In our analyses, no attempt was made to exclude the marked individuals from the (randomly) sampled individuals used for the cross sectional data set. The results we report are thus conservative regarding the benefits of integrating the datasets.

Section S2. Illustrative empirical example

To illustrate the novel approach we present here, we applied it to an empirical example. We considered the case of serotine bats (*Eptesicus serotinus*) exposed to a bat rabies virus (European Bat Lyssavirus type 1; EBLV-1) in Pagny-sur-Moselle, France (Robardet et al. 2017). Because there is no available dataset combining cross-sectional and capture-recapture setups to our knowledge, we chose to use this capture-recapture dataset and to simulate additional cross-sectional data using the simulation model presented above and parameterized based on the demographic and epidemiological parameters estimated using a mutlievent model. We used the longitudinal data presented in Robardet et al. 2017. We focus our analysis on one site only (Pagny-sur-Moselle) and on one age class only (adults). The cross-sectional data were simulated as explained in the main text. We then considered the model selected in Robardet et al. 2017. In this model, the survival, seroconversion, seroreversion and recapture probabilities are constant over time. In contrast, the resighting probability varies among sampling occasions. We considered this scenario when fitting the integrated model. The capture matrix fitted to the longitudinal data was thus written as time dependent (see codes in Appendix S7).

Section S3. Performances of the estimators

Dependence of the estimated parameters

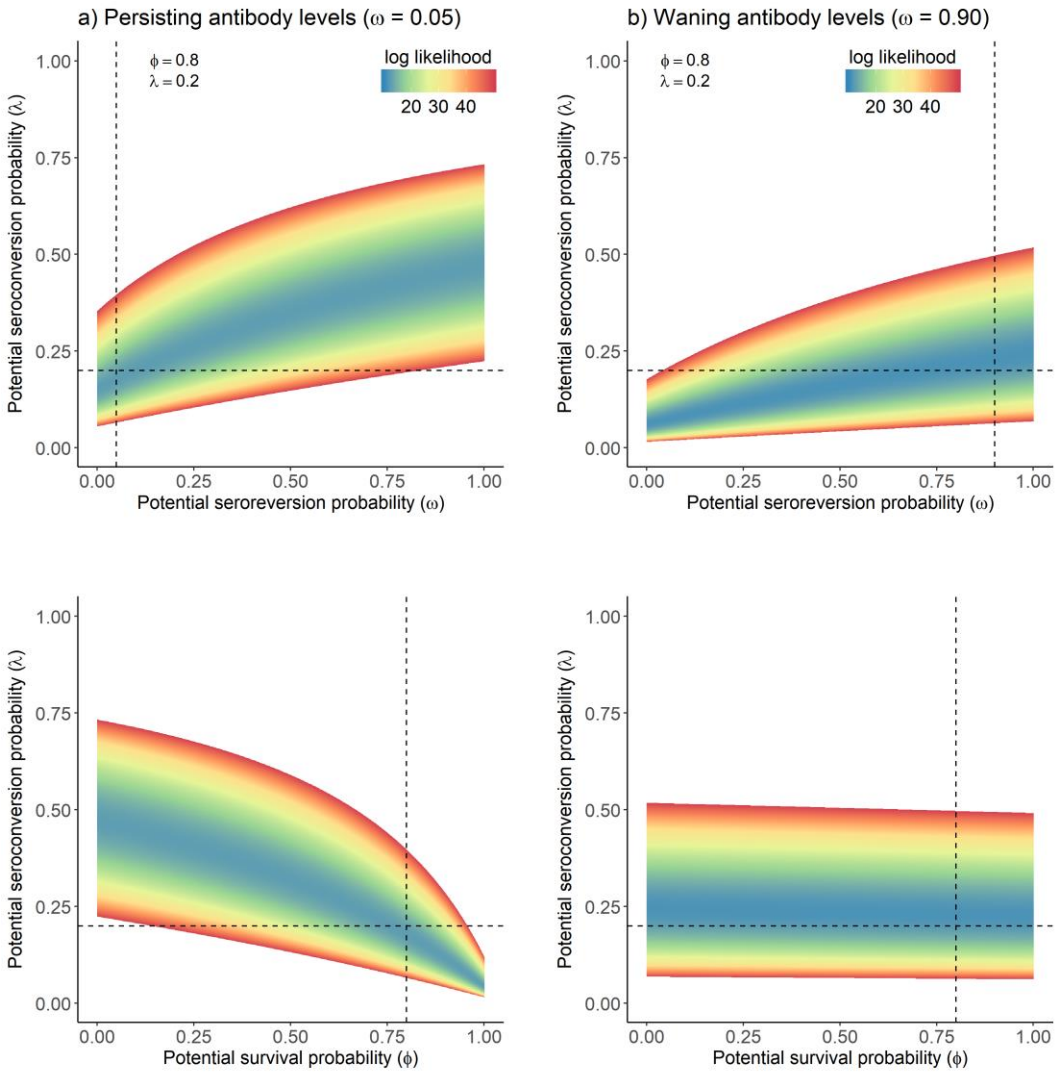

FIGURE S3. Profile negative log-likelihood of the cross-sectional estimator of the seroconversion probability (λ) when the seroreversion (ω) or the survival (ϕ) probabilities are not known. Overall, the less the seroprevalence a given year was dependent of the seroprevalence the previous year (*i.e.*, the lower was ϕ and the higher was ω), the better the cross-sectional estimator performs. This observation is easily explained by the fact that $\lim_{\phi \to 0} \pi^* = \lambda$ and $\lim_{\omega \to 1} \pi^* = \lambda$ (equation S2). For the simulations, *a priori* knowledge was put on the non-considered parameter that was fixed at its true value (ω on the top panels, ϕ on the bottom panels) and the negative log-likelihood is represented as a function of potential values for the two other parameters (λ and ϕ on the top panels and λ and ω on the bottom panels); dashed

lines indicate true parameter values. This figure illustrates that, for a given λ and a given ϕ, the cross-sectional estimator performance to accurately estimate λ at low ω (long antibody level persistence; a) is impeded by failure of the maximization of the likelihood. This failure was due to the likelihood being maximal for an erroneous value of λ for a majority of ϕ and ω potential values when cross-sectional models are not informed with *a priori* knowledge on these parameters. In contrast, for high values of ω (short antibody level persistence; b), the cross-sectional estimator offered a better performance. Survival similarly impacted the cross-sectional estimator performance, which is better for low ϕ (low survival).

Impact of eco-epidemiological parameters on the estimator performances

FIGURE S4 (p 17). Sensitivity of the cross-sectional and longitudinal estimators of the seroconversion probability (λ) to the survival (ϕ) and seroreversion (ω) probabilities based on cross-sectional (n_{CS} = 50; left panels) or longitudinal (n_{LG} = 50; right panels) data analyzed with non-informed models as an indicaton of the model dependency on *a priori* knowledge. For ϕ and ω, a set of values ranging from 0 to 1 was explored (with a step of 0.05) while λ and the observation parameters (p and δ) were fixed. The accuracy of an estimator is quantified by its MSE (a, b), a lower MSE indicating a better performance of the estimator. The MSE is decomposed into the bias (c, d) and the variance (e, f), highlighting that the high MSE (*i.e.*, poor performances) of the cross-sectional estimator for high ϕ and low ω is explained by the existence of a bias (see Fig. S3 for detailed explanations). Although ϕ and ω combinations for which the cross-sectional estimator is biased represent a small proportion of the parameter space, most epidemiological studies will fall in this range of values as long-lived host species are usually studied at the inter-annual scale (e.g., Chambert et al. 2012) and short-lived host species at shorter time scales (e.g., monthly time scale; Mariën et al. 2019).

FIGURE S5 (p 18). Sensitivity of the integrated estimator of the seroconversion probability (λ) to the survival (ϕ) and seroreversion (ω) probabilities based on cross-sectional (n_{CS} = 50) and longitudinal (n_{LG} = 50) data analyzed with non-informed models. For ϕ and ω, a set of values ranging from 0 to 1 was explored (with a step of 0.05) while λ and the observation parameters (p and δ) were fixed. The accuracy of an estimator is quantified by its MSE (a, b), a lower MSE indicating a better performance of the estimator. The MSE is decomposed into the bias (c, d) and the variance (e, f). The left and right panels represent the same data, but the left panels (a, c, e) use the same color scales as Fig. S4 for easier comparison of the different estimators, and the right panels (b, d, f) use an adapted color scales for easier visualization of subtle patterns. For instance, panel c illustrates that the integrated estimator is relatively unbiased (highest recorded bias value = 0.015) compared to the cross-sectional estimator (highest recorded bias value = 0.769; Fig. S4 c) for any ϕ and ω combination. In contrast, panel d illustrates that the integrated estimator is sensitive to ϕ and ω. In particular, higher bias values are observed for the ϕ = 1, ω = 0 combination (which corresponds to extreme values unlikely observed in natural systems), and for a range of low to intermediate ϕ values, corresponding to the parameter space where both the cross-sectional and longitudinal estimators performs relatively poorly (Fig. S4).

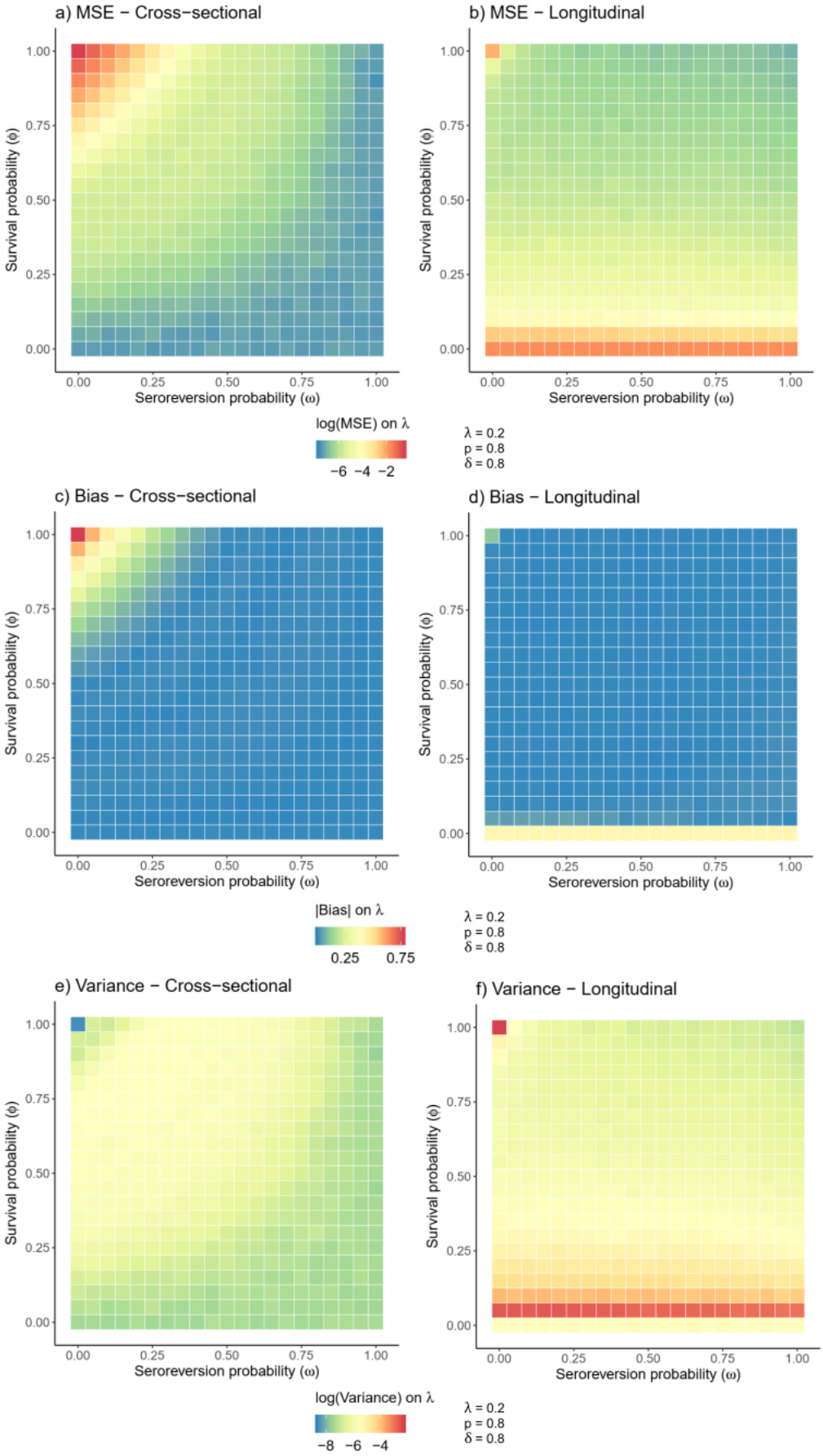
a) MSE − Cross−sectional
b) MSE − Longitudinal
c) Bias − Cross−sectional
d) Bias − Longitudinal
e) Variance − Cross−sectional
f) Variance − Longitudinal
Survival probability (ϕ)
Seroreversion probability (ω)
0.00
0.25
0.50
0.75
1.00
log(MSE) on λ
−6 −4 −2
|Bias| on λ
0.25 0.75
log(Variance) on λ
−8 −6 −4
λ = 0.2
p = 0.8
δ = 0.8

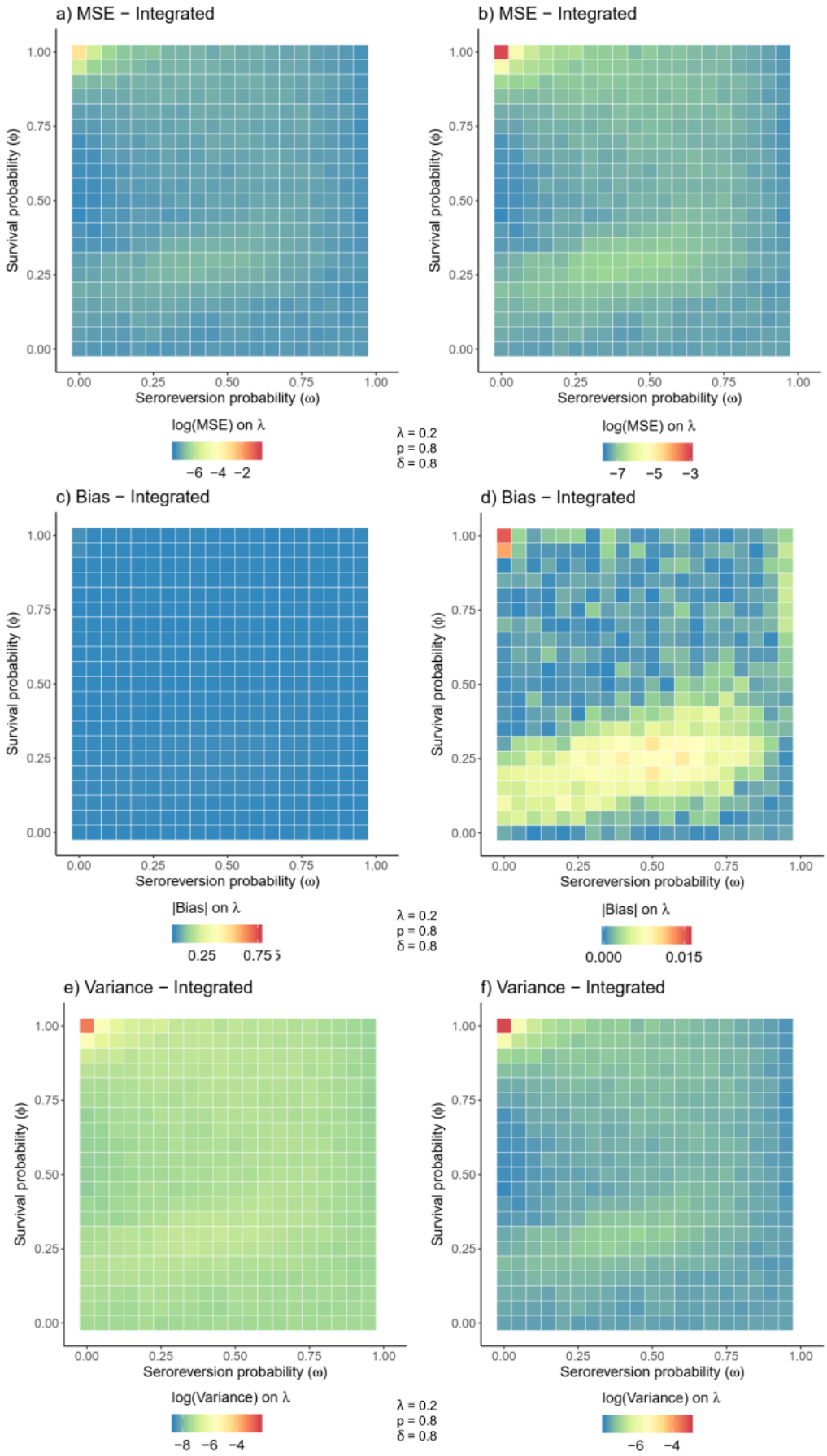
a) MSE − Integrated
b) MSE − Integrated
c) Bias − Integrated
d) Bias − Integrated
e) Variance − Integrated
f) Variance − Integrated
Survival probability (ϕ)
Seroreversion probability (ω)
0.00
0.25
0.50
0.75
1.00
log(MSE) on λ
−6 −4 −2
log(MSE) on λ
−7 −5 −3
|Bias| on λ
0.25 0.75
|Bias| on λ
0.000 0.015
log(Variance) on λ
−8 −6 −4
log(Variance) on λ
−6 −4
λ = 0.2
p = 0.8
δ = 0.8
λ = 0.2
p = 0.8
δ = 0.8
λ = 0.2
p = 0.8
δ = 0.8

Impact of observation parameters on the estimator performances

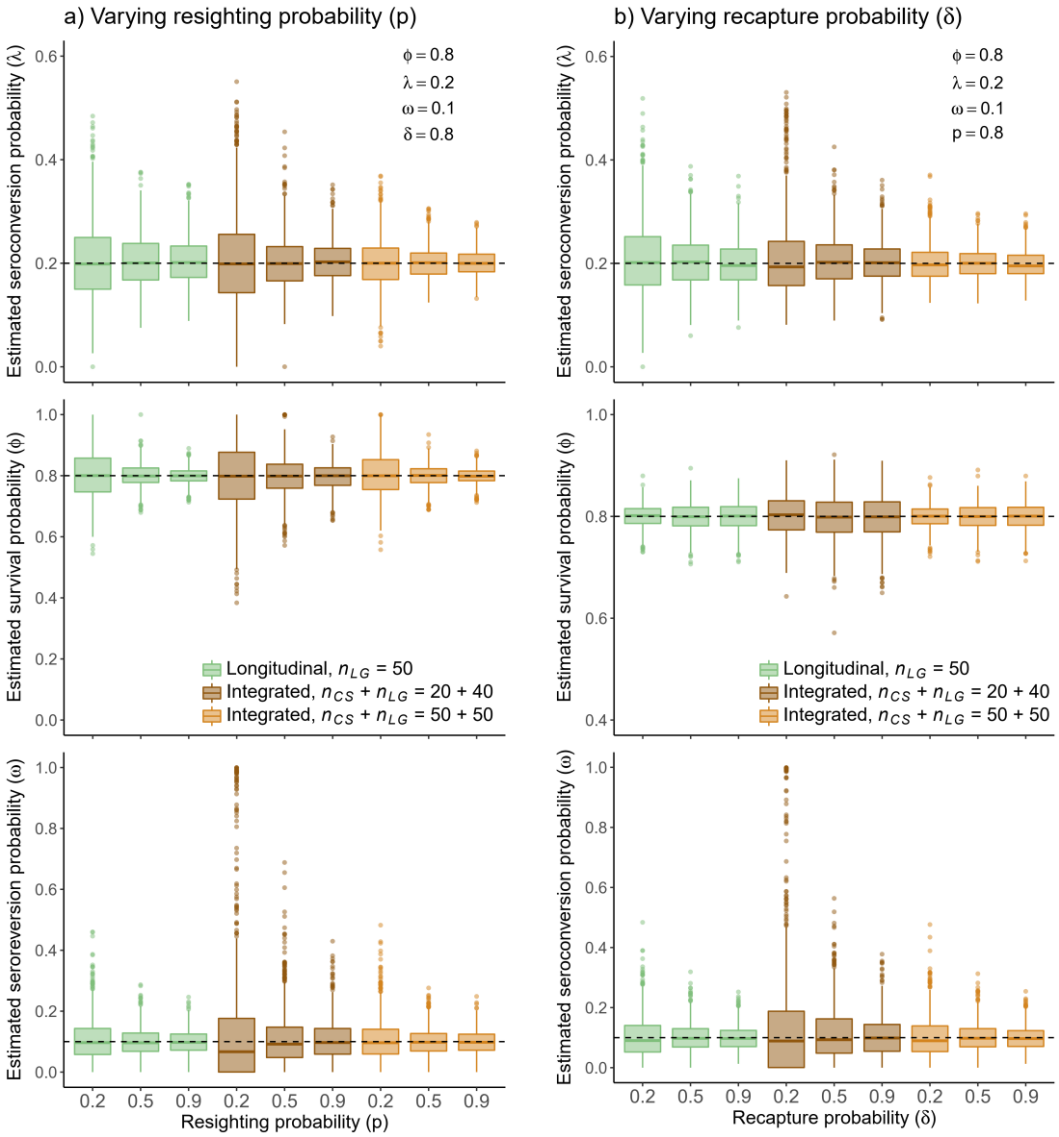

FIGURE S6. Effect of the resighting (p; a) and recapture (δ; b) probabilities on the estimation of the seroconversion (λ), survival (ϕ) and seroreversion (ω) probabilities. The true value of the estimated parameter is represented by a black dashed line. The samples sizes were chosen considering that the costs inherent to the capture of unmarked individuals are low to negligible (e.g., accidental capture or collaboration with harvesting or population control programs) compared to those of recapturing marked individuals. Note that the scale varies among the panels. As a reminder, resighting and recapture probabilities are defined as following: each year after the first year of the study, each alive marked individual is resighted with a probability p and its serological state is ascertained with a probability δ corresponding to the recapture probability after resighting (the serological state being ascertained at the same time from a blood sample). Hence, the probability to recapture a marked individual a year after it

has been marked is not equal to δ, but to $\phi \times p \times \delta$ (*i.e.*, it is still alive, it has been seen on the study site and capture attempt was successful). This probability is thus $\leq \delta$. The precision of the longitudinal and integrated estimators of seroconversion probability are impacted by these two observation parameters, the higher these parameters, the higher the precision of the estimators. The precision of the survival probability estimation is higher for higher resighting probabilities (a, middle). This result is expected considering that resighting only is sufficient to inform on the individual living state (alive *versus* dead) while (re)capture is necessary to assess the individual serological state (seronegative *versus* seropositive). In contrast, the precision of the survival probability estimation is lower for higher recapture probabilities in relation to the sampling protocol (b, middle). Indeed, the number of marked individuals captured each year (n_{LG}) is constant in the simulations. Thus, for low recapture probabilities a large number of individuals needs to be newly marked each year to maintain the number of yearly captured individuals at n_{LG}, increasing the total number of marked individuals (that can be resighted even if not recaptured) and thus the precision of the survival probability estimation.

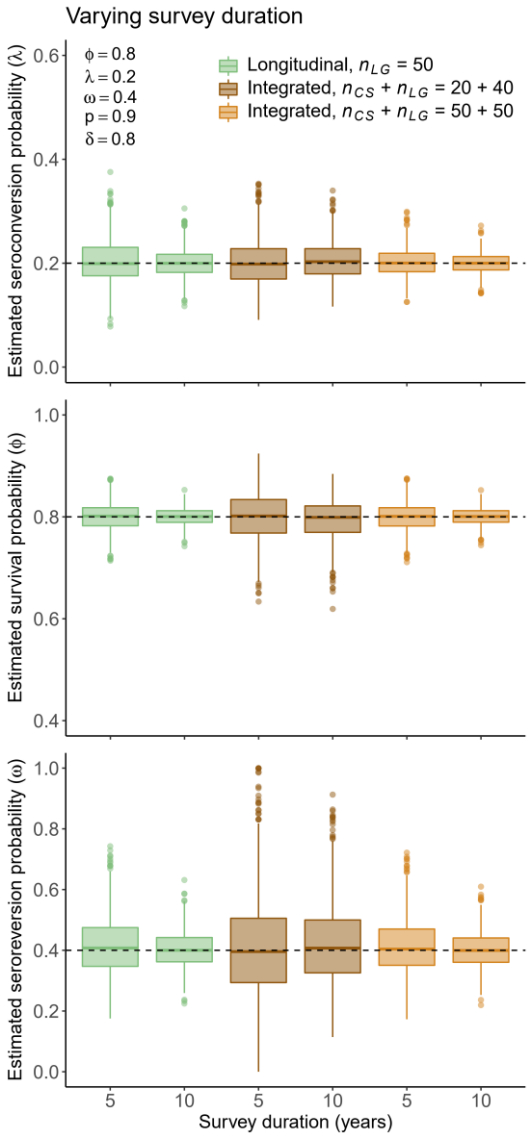

FIGURE S7. Effect of the survey duration on the estimation of the seroconversion (λ), survival (ϕ) and seroreversion (ω) probabilities. The true value of the estimated parameter is represented by a black dashed line. The samples sizes were chosen considering that the costs inherent to the capture of unmarked individuals are low to negligible (e.g., accidental capture or collaboration with harvesting or population control programs) compared to those of recapturing marked individuals. Note that the scale varies among the panels. The precision of the estimators was improved when the survey was conducted for ten years compared to five for all parameters.

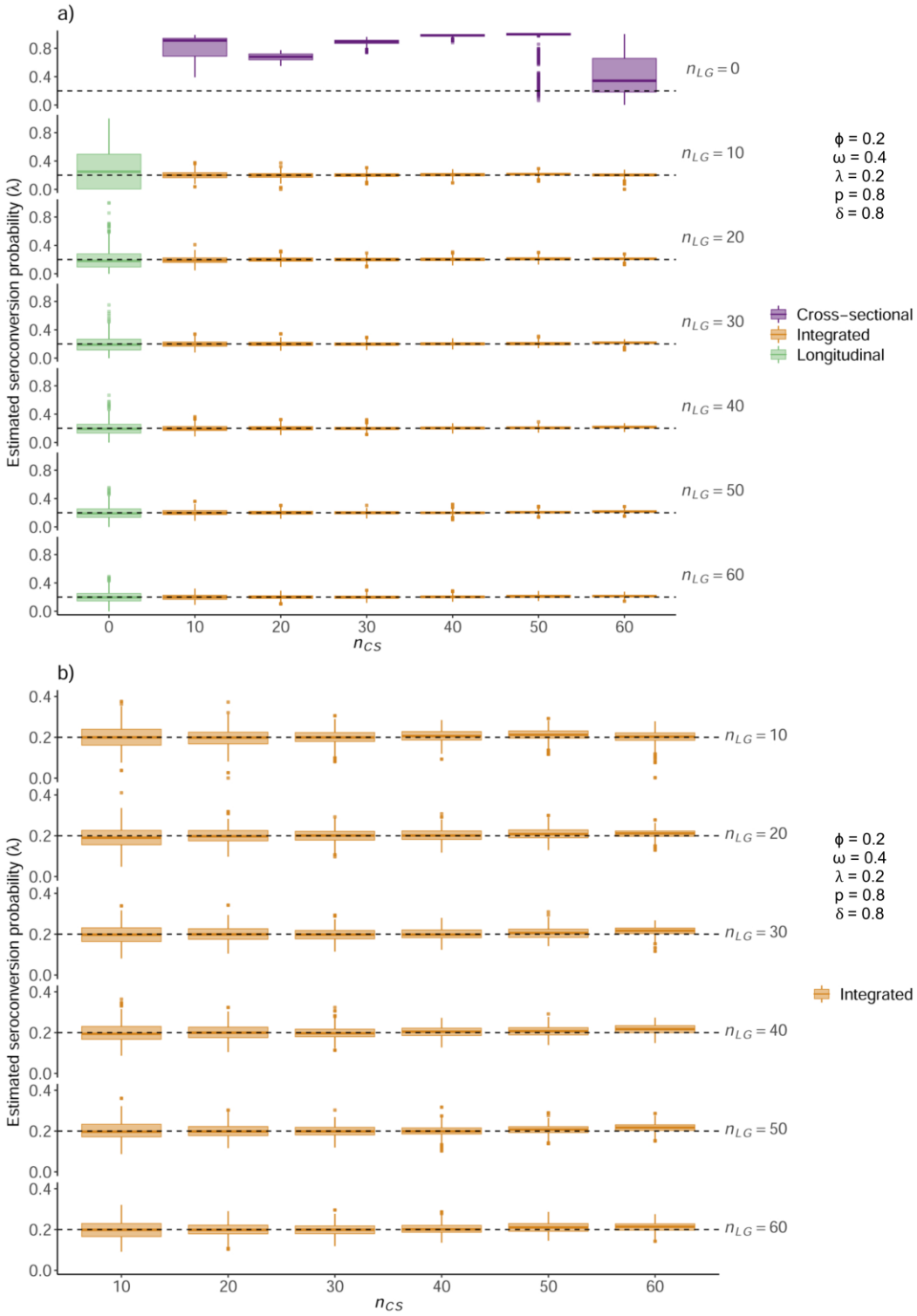

FIGURE S8. Effect of the sample size on the estimation of the seroconversion (λ) probability. The true value of the estimated parameter is represented by a black dashed line. Including a longitudinal sample to a cross-sectional sample (i.e., integrated design) allows to obtain an unbiased estimator. Panel b zooms on the integrated model outputs of panel a. A low value of the survival probability (ϕ = 0.2) was chosen

in order to be conservative regarding the potential benefits of the longitudinal and integrated models. In these conditions, using the integrated design, increasing the cross-sectional sample size improved the precision of the integrated estimator, while the effect of the longitudinal sample size appears relatively negligible. Note that the cross-sectional estimator is biased because not informed with any *a priori* knowledge on host survival (ϕ) and seroreversion (ω) probabilities (see Fig. 2 and S3 for more detailed explanations).

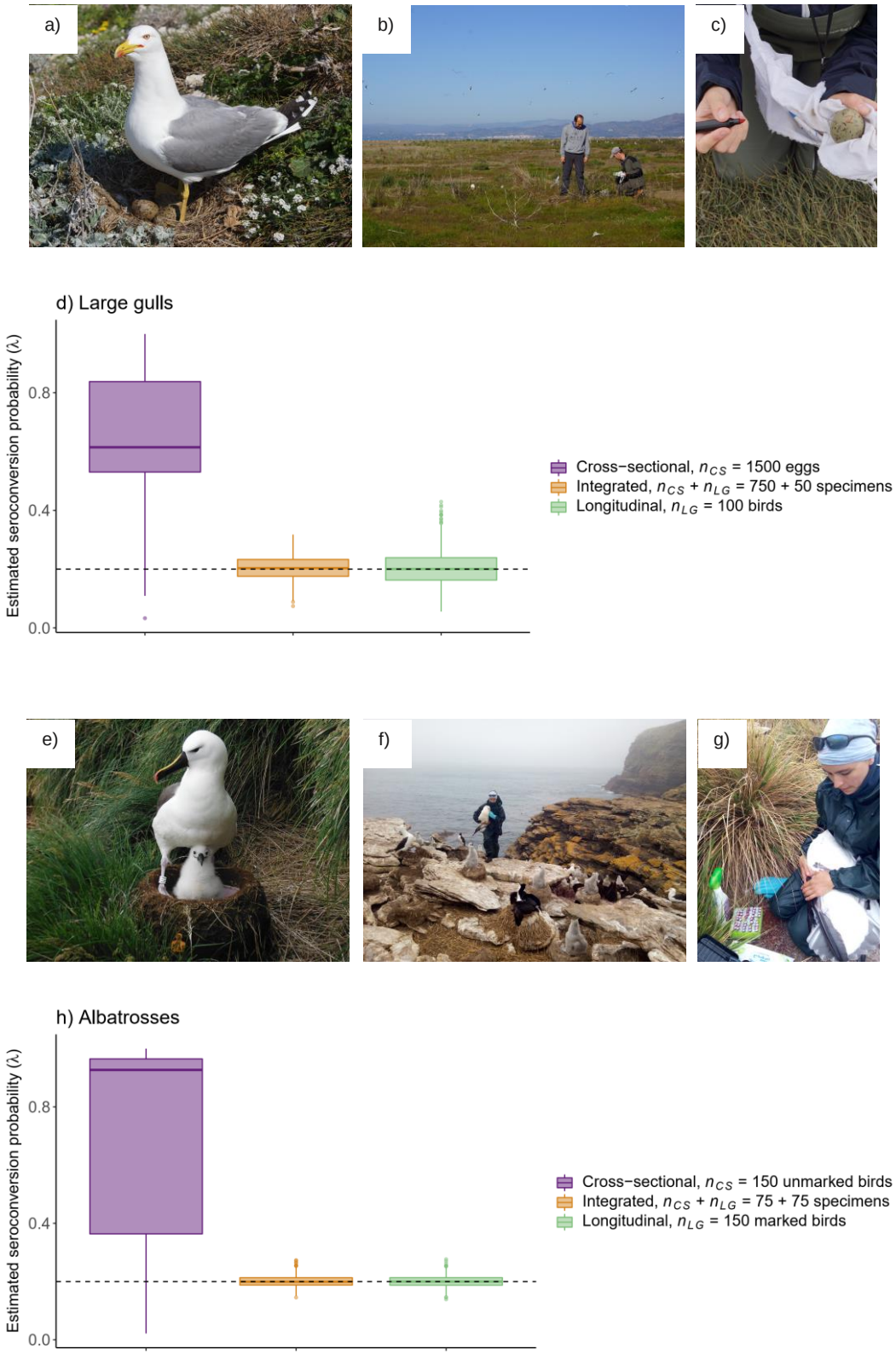

FIGURE S9. Illustrative cost analysis in two biological system: a yellow-legged gull (*Larus michahellis*) colony (top panels) and an Indian yellow-nosed albatross (*Thalassarche carteri*) colony (bottom panels).

The pictures represent the different steps of sample collection for the two types of species (observation, capture and sampling). The graphics represent the performances of the cross-sectional, integrated and longitudinal estimators of the seroconversion probabilities at constant time costs (15 days of field work per year). These two examples were selected to illustrate that the costs inherent to sample collection can greatly vary depending on the host species ecology (e.g., breeding site faithfulness, flight response to the presence of potential terrestrial predators…) and the capture methods (e.g., targeted versus non-targeted, manual versus use of tools…). For instance, although yellow-legged gulls and yellow-nosed albatrosses are both medium-size non-burrow nesting seabirds, they exhibit different ecologies and behaviours, with consequences on the costs of unmarked or marked specimen sampling. Albatrosses are highly faithful to their breeding sites, as a large proportion of individuals re-use the same nest year after year (e, notice the nest tag on the picture; relatively high resighting probability p). In contrast, large gulls build new nests every years, making it more difficult to track the same individuals at the inter-annual scale (relatively low resighting probability p). Regarding the capture itself, because they have long been isolated from terrestrial predators (Chapuis et al. 1994), many albatross populations lack anti-predation behaviour (Cresswell, 2010) and both adults and nestlings can be relatively easily captured by hand (f; relatively high recapture probability δ and intermediate cost of unmarked or marked individual sampling). In contrast, large gulls exhibit behaviour such as flight response to human presence (b), making it more difficult to capture adult individuals (relatively low recapture probability δ and high cost of marked specimen capture). However, their population is regulated by egg sterilisation at several locations, opening the possibility to collect egg yolk samples (c; instead of blood samples), which can be screened for maternal antibodies (see Appendix S1-D), with no additional impact on population dynamics. Hence, cross-sectional samples can be constituted by collected eggs (instead of capturing birds) in some large gulls populations (relatively low cost of unmarked specimen sampling); but such approaches cannot be implemented in albatross populations considering their breeding ecologies (only laying one egg per year or every two years depending on the species) and conservation statuses. In addition to their pedagogical interests, these two examples are particularly relevant as both large gulls and albatrosses are more and more subject to epidemiological studies. Yellow-legged gulls are suspected reservoirs or bridge hosts of several zoonotic infectious agents (e.g., Arnal et al. 2015; Vittecoq et al. 2016; Gamble et al. 2019b; Navarro et al. 2019), raising public health questions and representing potentially useful sentinels. In contrast, epidemiological studies conducted in albatrosses usually focus on the conservation issues raised by infectious diseases in these populations (e.g., Uhart et al. 2016; Bourret et al. 2018). The simulation parameters and the costs linked to the sampling of unmarked or marked specimens of the two species were estimated based on the field experience of the authors' team (e.g., Arnal et al. 2014; Hammouda et al. 2014; Garnier et al. 2017; Bourret et al. 2018; Gamble et al. 2019a, b) and the literature (Payo-Payo et al. 2015; Gamble et al. 2019a). Regarding the seroreversion

rate, an intermediate probability was chosen, representing for instance the dynamics of the specific immune response following exposure to the parasite *Toxoplasma gondii* (Sandström et al. 2013) or *Pasteurella multocida* bacteria (Gamble et al. 2019a). Note that the cross-sectional estimator is biased because not informed with any *a priori* knowledge host survival (ϕ) and seroreversion (ω) probabilities (see Fig. 2 and S3 for more detailed explanations). Overall, in large gulls, integrating cross-sectional and longitudinal samples can increase the accuracy of the seroconversion probability estimator compared to the longitudinal estimator (d), while in albatrosses, the longitudinal and integrated estimators perform equally (h). Note also that the longitudinal and integrated estimators are more precise in the albatross case than in the large gull case, due to the highest survival, resigthing and recaptures probabilities of albatrosses compared to large gulls (see Fig. S6).

a: a yellow-legged gull (*Larus michahellis*) on its eggs on Frioul Island (Parc National des Calanques, Mediterranean Sea). b: large gulls often take-off from their nests when approached by a potential predator, especially at the beginning of the breeding season, as illustrated here (Parc Natural del Delta de l'Ebre, Mediterranean coasts). c: sampling of a yellow-legged gull egg on Corrège Island (Etang de Leucate, Mediterranean coasts) for maternal antibody screening. e: a marked Indian yellow-nosed albatross (*Thalassarche carteri*) on its nestling on Amsterdam Island (Réserve Naturelle National des Terres Australes Françaises, Southern Indian Ocean). f: seabirds breeding on islands historically free of terrestrial predators can relatively easily be approached, for mark resighting or (re)capture, as they often do not fly away when approached by potential predators as illustrated here in a black-browed albatross (*Thalassarche melanophris*), imperial shag (*Leucocarbo atriceps*) and southern rockhopper penguin (*Eudyptes chrysocome*) colony on New Island (Falkland Islands, Southern Atlantic Ocean). g: preparation of the collection of a blood sample from a black-browed albatross on New Island (Falkland Islands, Southern Atlantic Ocean) for antibody screening. Pictures: © Thierry Boulinier (c), Thierry Boulinier / IPEV (e, f, g), Amandine Gamble (a, b), featuring Raul Ramos (b), Thierry Boulinier (b), Amandine Gamble (c, f, g).

Section S4. Discussion of egg sampling

In some situations, maternally transmitted antibodies can be detected in egg yolk or serum collected from newborns and represent an alternative source of information on breeding female exposure to infectious agents without requiring the sometime difficult capture of adults (Hammouda et al. 2014). Particularly efficient cross-sectional sampling designs could thus not even require the capture of adults if the sampling of offspring can be used as a reliable alternative to adult blood sampling. This alternative can allow practitioners to reasonably consider important sample sizes with considerably limited costs regarding necessary time, with the extreme case of egg sampling for birds and reptiles, when the sampling of partial clutches can allow inferring the amount of circulating antibodies of breeding females (e.g., Gasparini et al. 2001, Alekseeev et al. 2014, Arnal et al. 2014, Hammouda et al. 2014, Gamble et al. 2019b). Egg sampling can notably be considered for populations undergoing population controls and/or when the partial collection of clutches is not expected to affect significantly the breeding success. For instance, some large gull colonies have been undergoing egg sterilisation as part of other species conservation programs or to limit interactions with human populations (Oro & Martinez-Vilalta 1994; Belant 1997). Species subject to limitation are often abundant opportunistic feeders living close to human populations, potentially exposed to a wide range of infectious agents (e.g., Monaghan et al. 1985; Carlson et al. 2011; Arnal et al. 2015). They can thus constitute good sentinels for infectious agent monitoring at the human-wildlife interface (Halliday et al. 2007). Some simple rules could also allow sampling eggs with a limited demographic impact. For instance, in many avian species, replacement eggs will be laid if eggs are sampled soon after laying (e.g. Nager et al. 1999 in *Larus fuscus* gulls). When egg sampling is not practicable, it may be possible to collect blood from newborns, although special attention should be put on maternal immunity persistence and immune system development to be able to differentiate maternal antibodies from endogenous antibodies (Garnier et al. 2012, Saubusse et al. 2016).

Section S5. Recent advances in serology

Approaches based on serology can inform on individual past exposure to infectious agents. Their main advantages compared to direct detection of infectious agents (e.g., by PCR) are that (1) it is based on samples relatively easy to collect (blood, by opposition to tissues) and most importantly (2) it is informative even if individuals are sampled outside of the infectious period. This is especially the case when the infectious period is short and the antibody persistence long and/or when infection is asymptomatic, making it impossible to detect the infectious period without dedicated screening. However, serology does not inform on the current individual infectious status. Recent statistical frameworks explicitly address this question by allowing the time since infectious to be inferred from serological data (Borremans et al. 2016, Pepin et al. 2017). Despite requiring more field effort, the longitudinal monitoring of the serological state of marked individuals has the considerable benefits of allowing to detect status changes and to estimate directly key rates of change (Conn and Cooch 2009).

Another weakness of serology is the limited specify of the most common immunoassays. For instance, commercially available enzyme-linked immunosorbent assays (or ELISA) detecting antibodies directed against flaviviruses, notably West Nile Virus, usually do not discriminate among related flaviviruses. Additional samples or analyses are thus needed to characterize the circulating virus after detection of antibodies in the hosts with a broad ELISA assay, such as samples of a vector or to conduct more specific seroneutralisation assays (e.g., Arnal et al. 2014). However, recently developed tools now allow to extract more information from serology without increasing laboratory efforts, with for instance multiplex assays which can detect antibodies directed against several infectious agents simultaneously or discriminate among viral serotypes from small volumes of sample (Freidl et al. 2014, Beck et al. 2015).

Literature cited

Alekseeev, A. Y., K. A. Sharshov, V. Y. Marchenko, Z. Li, J. Cao, F. Yang, A. M. Shestopalov, V. A. Shkurupy, and L. Li. 2014. Antibodies to Newcastle Disease Virus in egg yolks of great cormorant (*Phalacrocorax carbo*) at Qinghai Lake. Advances in Infectious Diseases 04:194–197.

Arnal, A., E. Gómez-Díaz, M. Cerdà-Cuéllar, S. Lecollinet, J. Pearce-Duvet, N. Busquets, I. García-Bocanegra, N. Pagès, M. Vittecoq, A. Hammouda, B. Samraoui, R. Garnier, R. Ramos, S. Selmi, J. González-Solís, E. Jourdain, and T. Boulinier. 2014. Circulation of a Meaban-like virus in yellow-legged gulls and seabird ticks in the Western Mediterranean Basin. PLOS ONE 9:e89601.

Arnal, A., M. Vittecoq, J. Pearce-Duvet, M. Gauthier-Clerc, T. Boulinier, and E. Jourdain. 2015. Laridae: a neglected reservoir that could play a major role in avian influenza virus epidemiological dynamics. Critical Reviews in Microbiology 41:508–519.

Beck, C., P. Desprès, S. Paulous, J. Vanhomwegen, S. Lowenski, N. Nowotny, B. Durand, A. Garnier, S. Blaise-Boisseau, E. Guitton, T. Yamanaka, S. Zientara, and S. Lecollinet. 2015. A high-performance multiplex immunoassay for serodiagnosis of flavivirus-associated neurological diseases in horses. BioMed Research International 2015:1–13.

Belant, J. L. 1997. Gulls in urban environments: landscape-level management to reduce conflict. Landscape and Urban Planning 38:245–258.

Besbeas, P., S. N. Freeman, B. J. Morgan, and E. A. Catchpole. 2002. Integrating mark–recapture–recovery and census data to estimate animal abundance and demographic parameters. Biometrics 58:540–547.

Borremans, B., N. Hens, P. Beutels, H. Leirs, and J. Reijniers. 2016. Estimating time of infection using prior serological and individual information can greatly improve incidence estimation of human and wildlife infections. PLOS Computational Biology 12:e1004882.

Bourret, V., A. Gamble, J. Tornos, A. Jaeger, K. Delord, C. Barbraud, P. Tortosa, S. Kada, J.-B. Thiebot, E. Thibault, H. Gantelet, H. Weimerskirch, R. Garnier, and T. Boulinier. 2018.

Vaccination protects endangered albatross chicks against avian cholera. Conservation Letters 11:e12443.

Buzdugan, S. N., T. Vergne, V. Grosbois, R. J. Delahay, and J. A. Drewe. 2017. Inference of the infection status of individuals using longitudinal testing data from cryptic populations: towards a probabilistic approach to diagnosis. Scientific Reports 7:1111.

Carlson, J. C., R. M. Engeman, D. R. Hyatt, R. L. Gilliland, T. J. DeLiberto, L. Clark, M. J. Bodenchuk, and G. M. Linz. 2011. Efficacy of European starling control to reduce Salmonella enterica contamination in a concentrated animal feeding operation in the Texas panhandle. BMC veterinary research 7:9.

Chambert, T., V. Staszewski, E. Lobato, R. Choquet, C. Carrie, K. D. McCoy, T. Tveraa, and T. Boulinier. 2012. Exposure of black-legged kittiwakes to Lyme disease spirochetes: dynamics of the immune status of adult hosts and effects on their survival. Journal of Animal Ecology 81:986–995.

Chapuis, J. L., P. Boussès, and G. Barnaud. 1994. Alien mammals, impact and management in the French subantarctic islands. Biological Conservation 67:97–104.

Choquet, R., C. Carrié, T. Chambert, and T. Boulinier. 2013a. Estimating transitions between states using measurements with imperfect detection: application to serological data. Ecology 94:2160–2165.

Choquet, R., A. Sanz-Aguilar, B. Doligez, E. Nogué, R. Pradel, L. Gustafsson, and O. Gimenez. 2013b. Estimating demographic parameters from capture-recapture data with dependence among individuals within clusters. Methods in Ecology and Evolution 4:474–482.

Conn, P. B., and E. G. Cooch. 2009. Multistate capture-recapture analysis under imperfect state observation: an application to disease models. Journal of Applied Ecology 46:486–492.

Cresswell, W. 2010. Predation in bird populations. Journal of Ornithology 152:251–263.

Freidl, G. S., E. de Bruin, J. van Beek, J. Reimerink, S. de Wit, G. Koch, L. Vervelde, H.-J. van den Ham, and M. P. G. Koopmans. 2014. Getting more out of less – A quantitative

serological screening tool for simultaneous detection of multiple influenza A hemagglutinin-types in chickens. PLOS ONE 9:e108043.

Gamble, A., R. Garnier, A. Jaeger, H. Gantelet, E. Thibault, P. Tortosa, V. Bourret, J.-B. Thiebot, K. Delord, H. Weimerskirch, J. Tornos, C. Barbraud, and T. Boulinier. 2019a. Exposure of breeding albatrosses to the agent of avian cholera: dynamics of antibody levels and ecological implications. Oecologia. 189:939–949.

Gamble, A., R. Ramos, Y. Parra-Torres, A. Mercier, L. Galal, J. Pearce-Duvet, I. Villena, T. Montalvo, J. González-Solís, A. Hammouda, D. Oro, S. Selmi, and T. Boulinier. 2019b. Exposure of yellow-legged gulls to *Toxoplasma gondii* along the Western Mediterranean coasts: Tales from a sentinel. International Journal for Parasitology: Parasites and Wildlife 8:221–228.

Garnier, R., S. Gandon, K. C. Harding, and T. Boulinier. 2014. Length of intervals between epidemics: evaluating the influence of maternal transfer of immunity. Ecology and Evolution 4:568–575.

Garnier, R., R. Ramos, A. Sanz-Aguilar, M. Poisbleau, H. Weimerskirch, S. Burthe, J. Tornos, and T. Boulinier. 2017. Interpreting ELISA analyses from wild animal samples: some recurrent issues and solutions. Functional Ecology 31:2255–2262.

Garnier, R., R. Ramos, V. Staszewski, T. Militão, E. Lobato, J. González-Solís, and T. Boulinier. 2012. Maternal antibody persistence: a neglected life-history trait with implications from albatross conservation to comparative immunology. Proceedings of the Royal Society of London B: Biological Sciences 279:2033–2041.

Gasparini, J., K. D. McCoy, C. Haussy, T. Tveraa, and T. Boulinier. 2001. Induced maternal response to the Lyme disease spirochaete *Borrelia burgdorferi* sensu lato in a colonial seabird, the kittiwake *Rissa tridactyla*. Proceedings of the Royal Society of London B: Biological Sciences 268:647–650.

Gilbert, A. T., A. R. Fooks, D. T. S. Hayman, D. L. Horton, T. Müller, R. Plowright, A. J. Peel, R. Bowen, J. L. N. Wood, J. Mills, A. A. Cunningham, and C. E. Rupprecht. 2013. Deciphering serology to understand the ecology of infectious diseases in wildlife. EcoHealth 10:298–313.

Grosbois, V., P.-Y. Henry, J. Blondel, P. Perret, J.-D. Lebreton, D. W. Thomas, and M. M. Lambrechts. 2006. Climate impacts on Mediterranean blue tit survival: an investigation across seasons and spatial scales. Global Change Biology 12:2235–2249.

Lahoz-Monfort, J. J., G. Guillera-Arroita, and R. Tingley. 2016. Statistical approaches to account for false-positive errors in environmental DNA samples. Molecular Ecology Resources 16:673–685.

Hammouda, A., J. Pearce-Duvet, T. Boulinier, and S. Selmi. 2014. Egg sampling as a possible alternative to blood sampling when monitoring the exposure of yellow-legged gulls (*Larus michahellis*) to avian influenza viruses. Avian Pathology 43:547–551.

Halliday, J. E. ., A. L. Meredith, D. L. Knobel, D. J. Shaw, B. M. d. C. Bronsvoort, and S. Cleaveland. 2007. A framework for evaluating animals as sentinels for infectious disease surveillance. Journal of the Royal Society Interface 4:973–984.

Hénaux, V., M. D. Samuel, and C. M. Bunck. 2010. Model-based evaluation of highly and low pathogenic avian influenza dynamics in wild birds. PLOS ONE 5:e10997.

Hens, N., Z. Shkedy, M. Aerts, C. Faes, P. Van Damme, and P. Beutels. 2012. Modeling infectious disease parameters based on serological and social contact data: a modern statistical perspective. Springer Science & Business Media, New York.

Mariën, J., V. Sluydts, B. Borremans, S. Gryseels, B. Vanden Broecke, C. A. Sabuni, A. A. S. Katakweba, L. S. Mulungu, S. Günther, J. G. de Bellocq, A. W. Massawe, and H. Leirs. 2018. Arenavirus infection correlates with lower survival of its natural rodent host in a long-term capture-mark-recapture study. Parasites & Vectors 11:90.

Monaghan, P., C. B. Shedden, K. Ensor, C. R. Fricker, and R. W. A. Girdwood. 1985. Salmonella carriage by herring gulls in the Clyde Area of Scotland in relation to their feeding ecology. Journal of Applied Ecology 22:669–679.

Nager, R. G., P. Monaghan, R. Griffiths, D. C. Houston, and R. Dawson. 1999. Experimental demonstration that offspring sex ratio varies with maternal condition. Proceedings of the National Academy of Sciences 96:570–573.

Navarro, J., D. Grémillet, I. Afán, F. Miranda, W. Bouten, M. G. Forero, and J. Figuerola. 2019. Pathogen transmission risk by opportunistic gulls moving across human landscapes. Scientific Reports 9:10659.

Payo-Payo, A., D. Oro, J. M. Igual, L. Jover, C. Sanpera, and G. Tavecchia. 2015. Population control of an overabundant species achieved through consecutive anthropogenic perturbations. Ecological Applications 25:2228–2239.

Pepin, K. M., S. L. Kay, B. D. Golas, S. S. Shriner, A. T. Gilbert, R. S. Miller, A. L. Graham, S. Riley, P. C. Cross, M. D. Samuel, M. B. Hooten, J. A. Hoeting, J. O. Lloyd-Smith, C. T. Webb, and M. G. Buhnerkempe. 2017. Inferring infection hazard in wildlife populations by linking data across individual and population scales. Ecology Letters 20:275–292.

Ponchon, A., R. Choquet, J. Tornos, K. D. McCoy, T. Tveraa, and T. Boulinier. 2018. Survival estimates strongly depend on capture-recapture designs in a disturbed environment inducing dispersal. Ecography 41:255-266.

Ponchon, A., D. Grémillet, S. Christensen-Dalsgaard, K. E. Erikstad, R. T. Barrett, T. K. Reiertsen, K. D. McCoy, T. Tveraa, and T. Boulinier. 2014. When things go wrong: intra-season dynamics of breeding failure in a seabird. Ecosphere 5:art4.

Oro, D., and A. Martinez-Vilalta. 1994. Factors affecting kleptoparasitism and predation rates upon a colony of Audouin's gull (*Larus audouinii*) by yellow-legged gulls (*Larus cachinnans*) in Spain. Colonial Waterbirds 17:35–41.

Ramos, R., R. Garnier, J. González-Solís, and T. Boulinier. 2014. Long antibody persistence and transgenerational transfer of immunity in a long-lived vertebrate. The American Naturalist 184:764–776.

Robardet, E., C. Borel, M. Moinet, D. Jouan, M. Wasniewski, J. Barrat, F. Boué, E. Montchâtre-Leroy, A. Servat, O. Gimenez, F. Cliquet, and E. Picard-Meyer. 2017. Longitudinal survey of two serotine bat (*Eptesicus serotinus*) maternity colonies exposed to EBLV-1 (European Bat Lyssavirus type 1): Assessment of survival and serological status variations using capture-recapture models. PLOS Neglected Tropical Diseases 11:e0006048.

Rossi, S., M. Artois, D. Pontier, C. Crucière, J. Hars, J. Barrat, X. Pacholek, and E. Fromont. 2005. Long-term monitoring of classical swine fever in wild boar (*Sus scrofa* sp.) using serological data. Veterinary Research 36:27–42.

Rossi, S., C. Toigo, J. Hars, F. Pol, J.-L. Hamann, K. Depner, and M.-F. Le Potier. 2011. New Insights on the management of wildlife diseases using multi-state recapture models: the case of classical swine fever in wild boar. PLOS ONE 6:e24257.

Samuel, M. D., D. J. Shadduck, and D. R. Goldberg. 2005. Avian cholera exposure and carriers in greater white-fronted geese breeding in Alaska, USA. Journal of Wildlife Diseases 41:498–502.

Samuel, M. D., D. J. Shadduck, D. R. Goldberg, and W. P. Johnson. 2003. Comparison of methods to detect Pasteurella multocida in carrier waterfowl. Journal of Wildlife Diseases 39:125–135.

Sandström, C. A. M., A. G. J. Buma, B. J. Hoye, J. Prop, H. van der Jeugd, B. Voslamber, J. Madsen, and M. J. J. E. Loonen. 2013. Latitudinal variability in the seroprevalence of antibodies against *Toxoplasma gondii* in non-migrant and Arctic migratory geese. Veterinary Parasitology 194:9–15.

Saubusse, T., J.-D. Masson, M. Le Dimma, D. Abrial, C. Marcé, R. Martin-Schaller, A. Dupire, M.-F. Le Potier, and S. Rossi. 2016. How to survey classical swine fever in wild boar (*Sus scrofa*) after the completion of oral vaccination? Chasing away the ghost of infection at different spatial scales. Veterinary Research 47:21.

Uhart, M. M., L. Gallo, and F. Quintana. 2017. Review of diseases (pathogen isolation, direct recovery and antibodies) in albatrosses and large petrels worldwide. Bird Conservation International 28:169–196.

Vittecoq, M., S. Godreuil, F. Prugnolle, P. Durand, L. Brazier, N. Renaud, A. Arnal, S. Aberkane, H. Jean-Pierre, M. Gauthier-Clerc, F. Thomas, and F. Renaud. 2016. Antimicrobial resistance in wildlife. Journal of Applied Ecology 53:519–529.

Williams, B. K., J. D. Nichols, and M. J. Conroy. 2002. Analysis and management of animal populations: modeling, estimation, and decision making. Academic Press, San Diego, Calif.